Vision-based Inspection Algorithm for Identifying the Carbide Phase State in 12CrMoV Steel

Alexander Tzokev
Theory of Mechanisms and Machines
Technical University of Sofia
Sofia, Bulgaria
alextz@tu-sofia.bg

Anton Mihaylov
Materials Science and Technology
Technical University of Sofia
Sofia, Bulgaria
amm@tu-sofia.bg

Irina Topalova
Automation of Discrete Production Engineering
Technical University of Sofia
Sofia, Bulgaria
itopalova@tu-sofia.bg

Tzanko Georgiev
Industrial Automation
Technical University of Sofia
Sofia, Bulgaria
tzg@tu-sofia.bg

Abstract—**The paper presents a vision-based inspection algorithm for identifying the carbide phase state in 12CrMoV steel microstructures. The algorithm uses image preprocessing, anisotropic segmentation, discriminant analysis and mathematical model for calculating the residual life of the material. Based on the state of the carbide phase, the residual life can be precisely calculated. By implementing automated vision inspection, the subjective evaluation of microstructures by experts will be avoided.**

Keywords-vision inspection; discriminant analysis; steel microstrucutres; carbide phase; 12CrMoV steel

I. INTRODUCTION

The properties and the residual life of many types of steels (heat-resistant steels, tool steels, high strength steels, etc.) depend on the carbide phase, the quantity and the type of carbides, their shape and distribution. The state of the carbide phase is defined by heat treatment and can be altered by the working conditions [1,2].

The 12CrMoV steel pipes are used in thermal power plants for building superheaters with working temperature of up to 580°C. The microstructure of the metal alters (the properties of the material degrade) during exploitation based on the working temperature and the applied pressure. Visual analysis by experts shows that the carbide state in the microstructure is modified during the exploitation of the metal. This alteration is the main assessment factor for the structural state of the material and standard scales are used. The analysis is performed mainly by experts and consists in comparing the analyzed and standard scale images. This evaluation is subjective, uses a qualitative rather than a quantitative method and the results depend on the expert's qualification level, competence and experience [1,3,4].

At the moment, there are no integrated systems for performing this assessment. Some companies offer partial software and hardware solutions.

The microstructure state and the level of spheroidization (carbide phase) are used for calculating the time remaining until metal destruction - the residual life of the material. An automated carbide phase vision-based inspection algorithm (CPVBIA) will minimize the subjective evaluation and will help the experts in making their final decision for the residual life of the material. The CPVBIA applies quantitative assessment methods for achieving a qualitative result.

Fig. 1 shows the structural alterations of the 12CrMoV steel and the corresponding level of the spheroidization based on the adopted standards [1,3].

The photos in Fig. 1 show a metal structure with ferrite (bright zones) and carbide phases (dark zones and grains). Level 1 corresponds to new material and level 5 corresponds to a material with exhausted residual life which must be replaced.

The presented CPVBIA is based only on computer vision algorithms without implementing any adaptive technologies such as neural networks, genetic algorithms or fuzzy logic. The presented approach has 4 general stages, as shown in Fig. 2.

Level 1 — Lowest level of spheroidization
Level 5 — Highest level of spheroidization
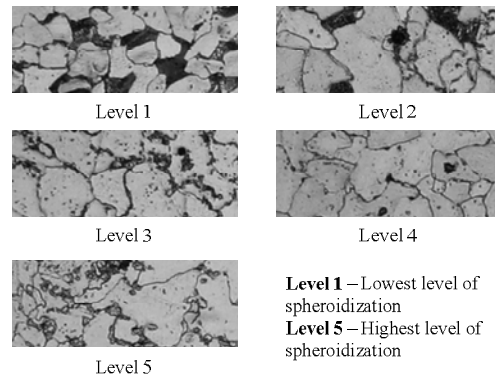
Figure 1. Level of spheroidization in 12CrMoV steel microstructures.
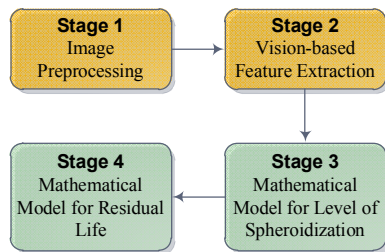
Figure 2. General stages of the CPVBIA

The first stage contains the entire image preprocessing - image resizing, converting to grayscale, filtration, etc. In stage 2, vision algorithms are applied for extracting crystallite borders and for identifying interesting zones that may contain the carbide phase. The result from the second stage is an array of 5 different morphological parameters for the carbide phase. In stage 3, a mathematical model based on morphological parameters is used to define the level of spheroidization. The final fourth stage calculates the residual life of the material based on external variables (working pressure and working time), the calculated carbide phase level and mathematical model of linear approximation, derived from CTO 1723082.100.005-2008 [1].

100 sample images (20 for each level of spheroidization) were used in the study. All of these images were analyzed and classified by experts.

II. IMAGE PREPROCESSING (STAGE 1)

In this study, all input images are acquired by digital microscope camera with 2Mpix resolution. If the input image is not a grayscale one, then color to grayscale conversion is applied.

The time needed for anisotropic segmentation (cf. III. Vision-based feature extraction) depends on the size of the input images. Therefore, in order to achieve higher performance, the algorithms in stage 1 resize the input image to 800x600 pixels if the original image is larger than that. To determine the relation between the size of the input image and the achieved recognition accuracy, a separate study can be conducted. An empirical analysis shows that 800x600 pixels are sufficient for fast and reliable feature extraction.

In general, stage 1 has only two steps:
1. Grayscale conversion
2. Image resizing

III. VISION-BASED FEATURE EXTRACTION (STAGE 2)

The second stage of CPVBIA extracts features from the image for further analysis and calculation of the spheroidization level. The extracted set of features must identify the carbide phase precisely and provide numerical data for stage 3. Two general types of features are extracted:
1. Crystallite borders
2. Interesting zones possibly containing carbide phase blobs

Fig. 3 shows the analyzed image, the interesting zones and the extracted borders of the grains.

a) Analyzed image   b) Extracted border

c) Interesting zones   d) Merged image
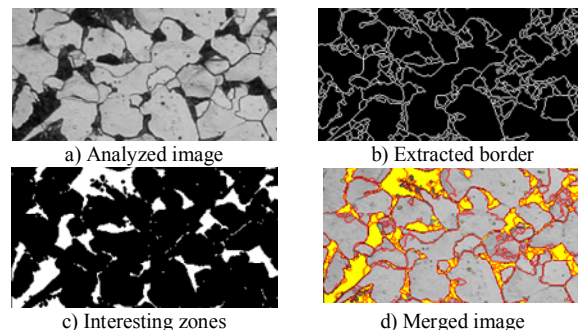
Figure 3. General stages of the CPVBIA

A. Extracting borders of the crystallites

To extract the borders of the grains after the image preprocessing, an anisotropic segmentation algorithm is applied. This segmentation algorithm is based on the method proposed by Malik [5]. This algorithm can segment grayscale images in disjoint regions of coherent brightness and contrast. Contours are treated in the intervening contour framework, while texture is analyzed using textons. Each of these cues has a domain of applicability, so to facilitate cue combination the authors introduce a gating operator based on the texturedness of the neighborhood at a pixel. Having obtained a local measure of how likely two nearby pixels are to belong to the same region, the algorithm uses the spectral graph theoretic framework of normalized cuts to find partitions of the image into regions of coherent texture and brightness [5].

Two parameters are used for the anisotropic filtration - the threshold K and the number of iteration (I). Fig. 4 shows blob extraction with different values for K and I. Experiments show that the best border extraction is achieved when K=2 and I=500.

After the anisotropic segmentation, a connected component labeling is applied for blob detection. The majority of the borders are connected so the biggest blob is extracted.

Analyzed image   K=2 I=500   K=2 I=10   K=2 I=100

K=2 I=1000   K=5 I=10   K=10 I=100
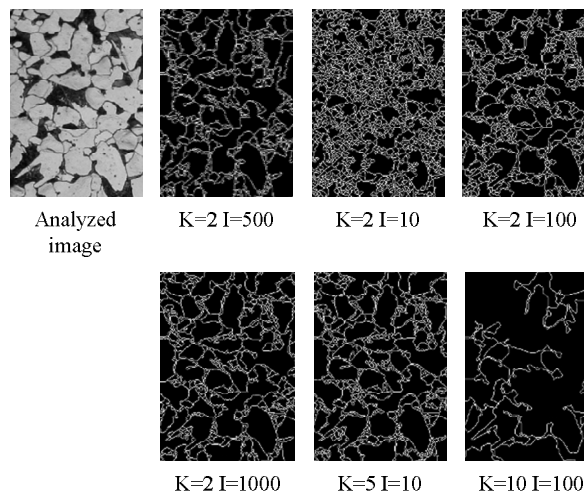
Figure 4. Border extraction with different values for K and I

B. *Extracting interesting zones*

To define the interesting zones that may contain the carbide phase, a Bradley local threshold algorithm [6] is applied to the analyzed image. This algorithm is a simple extension of Wellner's method [6] in which each pixel is compared to an average of the surrounding pixels and an approximate moving average of the last N pixels seen is calculated while traversing the image. If the value of the current pixel is T percent lower than the average, then it is set to black, otherwise it is set to white [6].

In the Bradley's algorithm, by using the integral image (also known as a summed-area table) instead of computing a running average of the last S pixels seen, the average of an SxS window of pixels centered on each pixel is calculated. This is a better average for comparison since it considers neighboring pixels on all sides. The average computation is accomplished in linear time by using the integral image [7].

A previous study shows that this algorithm is suitable for extracting the sigma phase and non-metal inclusions in austenitic stainless-steel microstructures [8]. The sigma phase has similar image features as the carbide phase for 12CrMoV steel. After the local threshold is applied, the resulting image is inverted and hit and miss filter is applied. The result is image containing the interesting zones.

A connected component labeling is used for blob detection. These blobs contain the carbide phase, noise in the image and other detected particles. To extract the sigma phase blobs from the noise, a simple filtration is applied – all blobs with height and width of the bounding rectangular less than 3 pixels are removed.

C. *Morphological parameters*

The result from stage 2 of the CPVBIA must be a numerical set of data describing the carbide phase. This data contains the following information for each blob:

1. Total number of blobs in the image.
2. Total area of the blobs in the image, measured in pixels.
3. Number of blobs inside the grains and on the borders.
4. Number of blobs on borders.
5. Average height of the bounding rectangular for all blobs, measured in pixels.
6. Average width of the bounding rectangular for all blobs, measured in pixels.
7. Average area of the blobs in the image.
8. Average fullness (area of the blob divided by the surface of the bounding rectangle) for all blobs in the image.
9. Average aspect (maximum of the height or width of the bounding rectangular, divided by the minimum of the height or width) for all blobs.

The numbers of blobs inside the grains and on the borders are used for final decision by the expert and are not used in stage 3. Fig. 5 shows subset analysis of the morphological parameters based on the sample images.
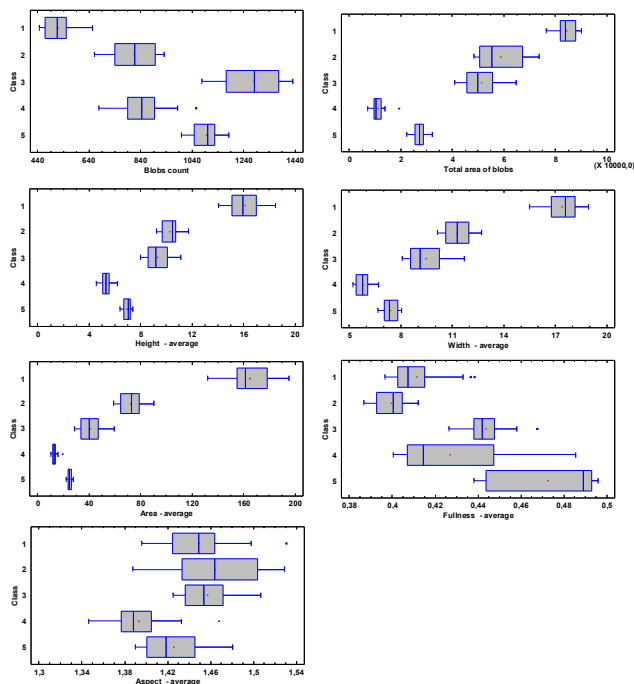
Figure 5. Subset analysis of the morphological parameters

The subset analysis shows that there is no only one morphological parameter that can classify the blobs. Each of the morphological parameters has some overlapping between the classes and a combination of two or more parameters should be used to correctly distinguish all 5 classes.

The summary statistics for the analyzed data is shown in Table I.

TABLE I.   SUMMARY STATISTICS FOR THE MORPHOLOGICAL PARAMETERS

Class	Count	Average	Standard Deviation	Coefficient of variation	Minimum	Maximum
1	20	517,6	59,5752	11,5099%	445,0	654,0
2	20	815,1	84,2514	10,3363%	661,0	932,0
3	20	1278,2	110,928	8,67849%	1079,0	1431,0
4	20	844,4	87,631	10,3779%	676,0	1056,0
5	20	1095,5	53,7181	4,90352%	998,0	1182,0
Total	100	910,16	273,071	30,0025%	445,0	1431,0

Class	Range	Standardized Skewness	Standardized Kurtosis
1	209,0	1,5628	0,374479
2	271,0	-0,583478	-0,914204
3	352,0	-0,170449	-1,11532
4	380,0	0,821561	0,695647
5	184,0	0,0152641	-0,919001
Total	986,0	0,0752718	-1,80172

IV. CALCULATING THE LEVEL OF SPHEROIDIZATION (STAGE 3)

A discriminant analysis based on the morphological data from 100 images was used to calculate the parameters for classification functions. Table II contains the classification function coefficients.

TABLE II.   CLASSIFICATION FUNCTION COEFFICIENTS

	1	*2*	*3*	*4*	*5*
C_{Blobs}	0,0280909	0,00172282	0,0926188	-0,020431	0,0405502
C_{Area}	-9,09884	-9,65378	-11,0216	-10,1958	-11,0222
C_{Height}	125,935	128,924	144,078	130,624	139,747
C_{Width}	112,696	95,9607	111,781	101,348	116,161
$C_{Fullness}$	5471,58	5255,23	5589,67	5561,88	5876,29
C_{Aspect}	2508,6	2701,41	2721,89	2861,86	2831,37
$C_{TotalArea}$	-0,0192403	-0,0185858	-0,0205796	-0,0208617	-0,0218383
CONST	-3382,34	-3338,62	-3729,97	-3632,74	-3909,51

$$y_{(i)} = CONST + C_{Blbos_i}.Blob\,Count + C_{Area_i}.Average\,area +$$
$$+ C_{Height_i}.Average\,height + C_{Width_i}.Average\,width +$$
$$+ C_{Fullness_i}.Average\,fullness + C_{Aspect_i}.Average\,aspect + \quad (1)$$
$$+ C_{TotalArea_i}.Total\,area$$

where $i = 1..5$ and the level of the spheroidization is calculated by (2).

$$Level\ of\ spheroidization = MAX(y_{(i)}) \quad (2)$$

The classification with prior probability of 0,2 for all levels is shown in Table III.

TABLE III.   CLASSIFICATION TABLE FOR DISCRIMINANT ANALYSIS

Actual Class	*Group Size*	*Predicted Class*				
		1	*2*	*3*	*4*	*5*
1	20	20	0	0	0	0
		(100,00%)	(0,00%)	(0,00%)	(0,00%)	(0,00%)
2	20	0	20	0	0	0
		(0,00%)	(100,00%)	(0,00%)	(0,00%)	(0,00%)
3	20	0	0	20	0	0
		(0,00%)	(0,00%)	(100,00%)	(0,00%)	(0,00%)
4	20	0	0	0	19	1
		(0,00%)	(0,00%)	(0,00%)	(95,00%)	(5,00%)
5	20	0	0	0	0	20
		(0,00%)	(0,00%)	(0,00%)	(0,00%)	(100,00%)

The summary statistics by each group is shown in Table IV.

TABLE IV.   SUMMARY STATISTICS BY GROUP

Class	1	2	3	4	5	TOTAL
COUNTS	20	20	20	20	20	100
MEANS						
Blobs count	517,6	815,1	1278,2	844,4	1095,5	910,16
Area average	164,978	72,2296	40,8611	13,0502	24,8825	63,2003
Height average	16,0838	10,282	9,30539	5,32764	6,94183	9,58813
Width average	17,3916	11,2668	9,46961	5,7954	7,3866	10,262
Fullness average	0,411401	0,3996	0,4436	0,427	0,4725	0,430824
Aspect average	1,44945	1,46447	1,45718	1,39305	1,42559	1,43795
Total area of blobs	84434,6	58818,1	51339,6	11120,6	27269,2	46596,4
STD. DEVIATIONS						
Blobs count	59,5752	84,2514	110,928	87,631	53,7181	273,071
Area average	18,5875	8,4545	8,95146	2,00407	1,61811	55,7795
Height average	1,20869	0,630084	0,90664	0,38898	0,2901	3,77871
Width average	1,04933	0,790887	1,04796	0,43678	0,43977	4,11296
Fullness average	0,012544	0,00770	0,00952	0,02654	0,02439	0,0311191
Aspect average	0,035857	0,042157	0,02393	0,02766	0,0278	0,0409149
Total area of blobs	3647,13	8959,74	7020,1	2638,28	2343,12	26143,4

Fig. 6 shows sample plots for some of the discriminant functions.
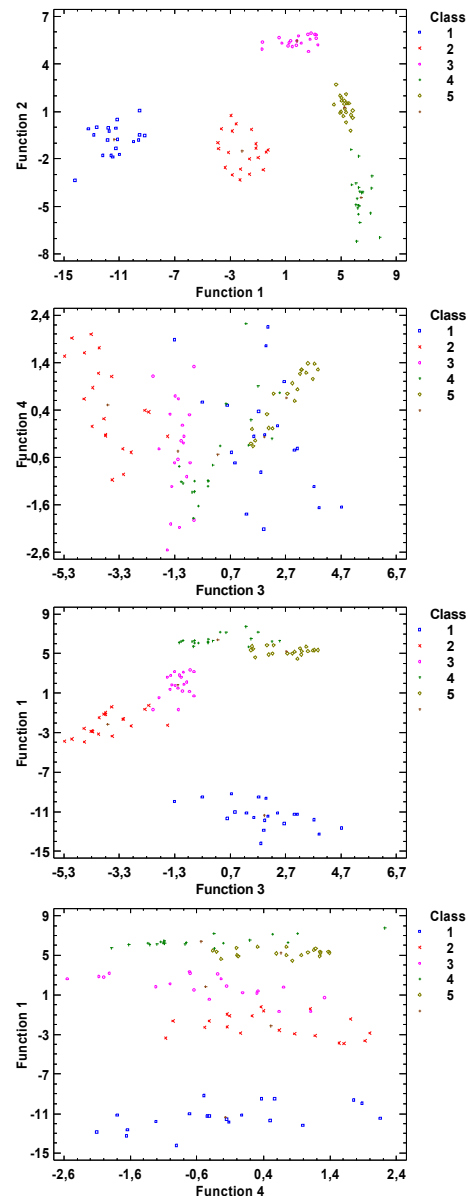
Figure 6. Classification functions

V.   CALCULATING THE RESIDUAL LIFE (STAGE 4)

The residual life is defined by the standard curves published in [1] and according to the same metallography standard several parameters are used to calculate this value:

1. Working hours
2. Nominal pressure
3. Level of spheroidization

As it was already defined, this analysis is subjective and highly dependent on the proficiency level of the expert. One of the main advantages of CPVBIA is removing the human factor.

From stage 3 the level of spherodization is calculated. By using linear approximation and the exponential equations from the nomograms the residual life can be precisely calculated avoiding the subjective factor.

VI. CPVBIA COMPLETE STRUCUTRE

The complete structure of the CPVBIA algorithm is shown in Fig. 7.
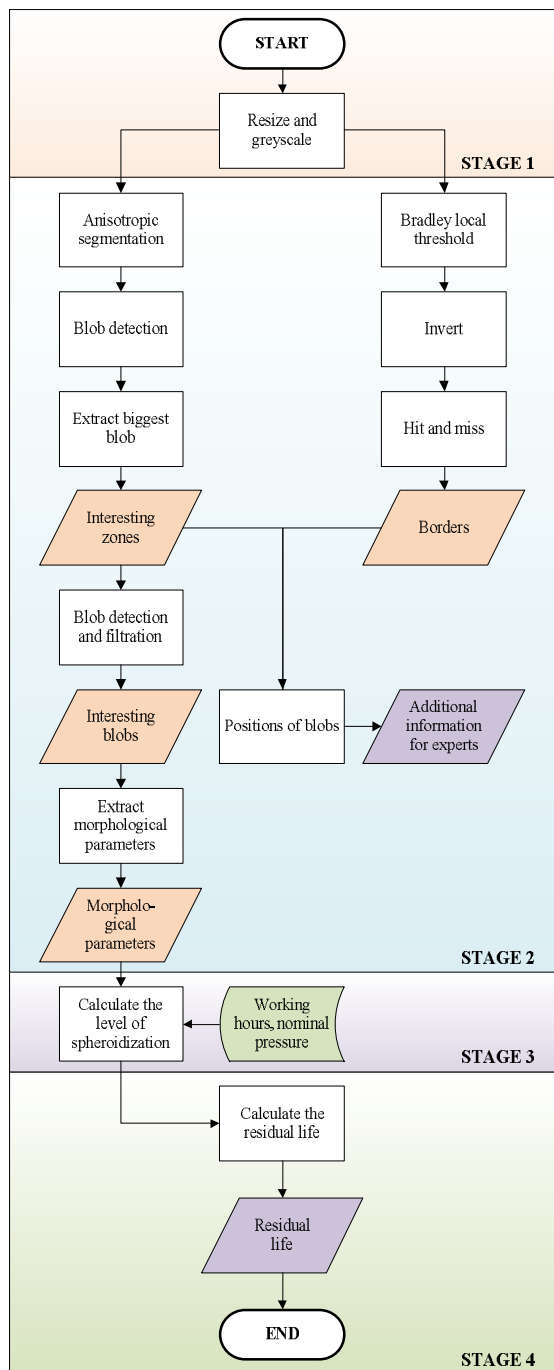
Figure 7. Complete structure of CPVBIA algorithm

VII. EXPERIMENTS AND RESULTS

To test and to validate the proposed algorithm, two groups of images were used. Group A contains images of steel microstructures of 12CrMoV steel for levels 1 to level 5. Group B contains images with varying contrast, microstructures of different steel type, larger optical magnification or insufficient preparation of the steel specimen. The results expected by experts are high classification accuracy within group A and high number of wrong classifications in group B.

All of the images in group A and group B were not used in the preliminary discriminant analysis.

Table V shows the results from the analysis.

TABLE V. EXPERIMENTAL DATA

Test Group	Description	Count	Correctly classified	Wrong classification
Group A	Level 1	8	8	0
	Level 2	13	10	3
	Level 3	6	5	1
	Level 4	18	18	0
	Level 5	11	10	1
Group B	Modified Contrast	4	0	4
	Different steel type	1	0	1
	Bigger optical magnification	8	0	8
	Not well developed borders	2	0	2
	Wrong amount of ferrite	1	0	1

Fig. 8 shows graphical representation for the classification accuracy in group A.
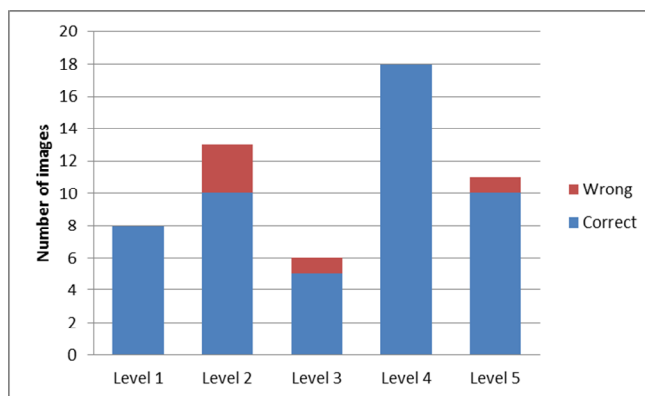
Figure 8. Recognition accuracy for group A

The classification accuracy for group A is 91.07% and 0.00% for group B, and these results confirm the expectations of experts. According to CTO 1723082.100.005-2008, the calculation of the carbide phase should be made on multiple microstructure images from the same steel exemplar [1].

Further analysis shows that two of the wrongly classified images in group A contain high amount of non-metal inclusion in the material, and one image has blurred zones. To improve the recognition accuracy, some images with small amount of non-metal inclusions can be added to the discriminant analysis for each level.

A detailed analysis of the algorithm parameters for group B shows that the error percentage between the correct level (classified by an expert) and the wrong level (classified by the CPVBIA) varies depending on the image type. Table VI contains the average of the classification functions and Δy (see (3)).

$$\Delta y = y_{Correct} - y_{Wrong} \qquad (3)$$

TABLE VI.   EXPERIMENTAL DATA FOR GROUP B

Description	Classification function - average					Avg ΔY
	y1	y1	y2	y4	y5	
Modified contrast	817.23	845.71	855.76	857.18	857.73	-1.41
Different steel type	1025.8	1025.4	1028.1	1035.5	1041.5	-15.70
Bigger optical magnification	896.90	916.76	919.90	928.95	929.74	-7.32
Poorly developed borders	903.46	919.47	921.56	928.56	931.1	-4.24
Wrong amount of ferrite	1109.8	1104.4	1110.4	1117.4	1126.3	-16.50

If the algorithm is used in an application, two of the most common problems with the input images will be the different contrast and the borders development. The contrast may vary due to different light conditions and the camera – Fig. 9a. Improper preliminary preparation and polishing of the steel specimen can lead to blurred or missing borders of the crystallites (see Fig. 9b).
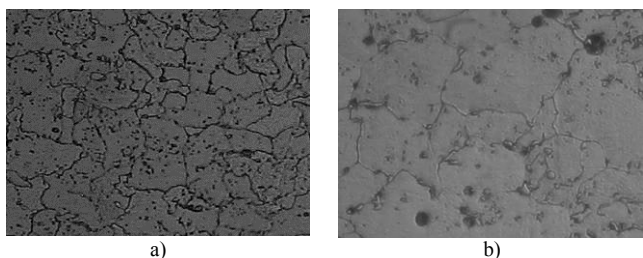
a)   b)
Figure 9. Input images with dissimilar contrast (a) and with poorly developed borders (b)

The Δy for these two types of images is low. If the images used in the discriminant analysis contain samples with varying contrast and poorly developed borders, the overall classification accuracy of the algorithm can be increased.

The analysis time for a single test image with the proposed algorithm parameters is around 170 seconds and depends on the hardware used. The slowest function is the anisotropic segmentation. By modifying the K and decrementing the number of iterations (cf. III, part A) the algorithm will be faster. In this type of analysis the overall inspection time is not important, but faster execution will allow the usage of the CPVBIA in more complex systems.

If a faster execution time is required (for application in real-time systems), an adaptive approach can be adopted. In this case the CPVBIA can be used in parallel for later validation or comparison of the results.

VIII.   CONCLUSIONS

A vision-based inspection algorithm for identifying the carbide phase and calculating the level of spheroidization in 12CrMoV is developed.

The algorithm is stable and the calculation accuracy for the carbide phase is very high – 91.07% (based on experiments).

The algorithm can be used in automated applications for carbide phase identification and calculation of the residual life of the material.

The overall execution time is slow due to the large number of iterations in the anisotropic segmentation function.

The CPVBIA can be used in parallel with adaptive approach (neural network) for result comparison.

Future studies can be performed with high resolution images and the algorithm can be tested for real-time application.

REFERENCES

[1] CTO 1723082.100.005-2008, Russia, 2008.

[2] I. Savova, N. Petrov, "Vacuum Heat Treatment of Tool Steels and Its Impact on the Operational Qualities of the Tools", Academic Open Internet Journal, Vol. 8, 2002.

[3] DL/T 773-2001, Spheroidization evaluation standard of 12Cr1MoV steel used in power plants, 2002.

[4] "ASM Handbook – Metallography and Microsotructures", Volume 9, ASM, USA, 2004.

[5] J. Malik, S. Belongie, T. Leung and J. Shi, "Contour and Texture Analysis for Image Segmentation", Internationa Journal of Computer Vision 43(1), Kluwer, Academic Publishers, Netherlands, pp. 7-27.

[6] A. Wellner, "Adaptive thresholding for the digitaldesk", Tech. Rep. EPC-93-110, EuroPARC, 1993.

[7] D. Bradely and G. Roth, "Adaptive Thresholding Using the Integral Image", Journal of Graphics Tools, A K Peters Ltd, Vol 12, USA, pp. 13-22.

[8] A. Tzokev, I. Topalova, and A. Mihaylov, "Adaptive Approach for Filtering the Sigma Phase in Austenitic Stainelss Steel Metallographic Mictrostructures", Mediterranean Conference on Control and Automation, Greece, 2011, pp. 1259-1264.